JACS
JOURNAL OF THE AMERICAN CHEMICAL SOCIETY
Article
pubs.acs.org/JACS

Stable Alkanes Containing Very Long Carbon–Carbon Bonds

Andrey A. Fokin,*[,⊥,‡] Lesya V. Chernish,[⊥] Pavel A. Gunchenko,[⊥] Evgeniya Yu. Tikhonchuk,[⊥] Heike Hausmann,[‡] Michael Serafin,[§] Jeremy E. P. Dahl,[∥] Robert M. K. Carlson,[∥] and Peter R. Schreiner*[,‡]

[⊥]Department of Organic Chemistry, Kiev Polytechnic Institute, pr. Pobedy 37, 03056 Kiev, Ukraine

[‡]Institute of Organic Chemistry, Justus-Liebig University, Heinrich-Buff-Ring 58, D-35392 Giessen, Germany

[§]Institut für Anorganische Chemie der Justus-Liebig-Universität, Heinrich-Buff-Ring 58, D-35392 Giessen, Germany

[∥]Stanford Institute for Material and Energy Science, Geballe Lab for Advanced Materials, Stanford University, Stanford, California 94305, United States

Supporting Information

ABSTRACT: The metal-induced coupling of tertiary diamondoid bromides gave highly sterically congested hydrocarbon (hetero)dimers with exceptionally long central C–C bonds of up to 1.71 Å in 2-(1-diamantyl)[121]tetramantane. Yet, these dimers are thermally very stable even at temperatures above 200 °C, which is not in line with common C–C bond length versus bond strengths correlations. We suggest that the extraordinary stabilization arises from numerous intramolecular van der Waals attractions between the neighboring H-terminated diamond-like surfaces. The C–C bond rotational dynamics of 1-(1-adamantyl)diamantane, 1-(1-diamantyl)diamantane, 2-(1-adamantyl)triamantane, 2-(1-diamantyl)triamantane, and 2-(1-diamantyl)[121]-tetramantane were studied through variable-temperature ^{1}H- and ^{13}C NMR spectroscopies. The shapes of the inward (*endo*) CH surfaces determine the dynamic behavior, changing the central C–C bond rotation barriers from 7 to 33 kcal mol^{-1}. We probe the ability of popular density functional theory (DFT) approaches (including BLYP, B3LYP, B98, B3LYP-D*n*, B97D, B3PW91, BHandHLYP, B3P86, PBE1PBE, wB97XD, and M06-2X) with 6-31G(d,p) and cc-pVDZ basis sets to describe such an unusual bonding situation. Only functionals accounting for dispersion are able to reproduce the experimental geometries, while most DFT functionals are able to reproduce the experimental rotational barriers due to error cancellations. Computations on larger diamondoids reveal that the interplay between the shapes and the sizes of the CH surfaces may even allow the preparation of open-shell alkyl radical dimers (and possibly polymers) that are strongly held together exclusively by dispersion forces.

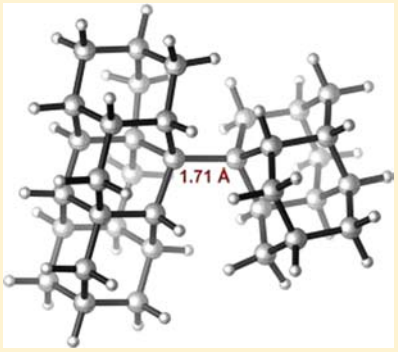

INTRODUCTION

A distance of 1.54 Å is considered an average value for an unstrained alkane C–C bond.[1] Experimentally known deviations from this value typically lie within less than 10% but this seemingly small variation from the ideal bond length leads to large differences in the relative stabilities of hydrocarbons.[2] Generally, it is believed (but not physically founded[3]) and expressed in textbooks that longer C–C bonds are weaker, that is, an inverse correlation exists between the bond lengths and bond dissociation energies (BDEs).[2] For instance, the rates for homolytic cleavage of the C–C bond estimated[4] for ethane and hypothetical hexaphenyl ethane (**1**, Figure 1) differ by a factor of 10^{30}, representing the most remarkable substituent effect in chemistry. This underlines the instability of **1**: Its central CC bond is simply too weak as well as "too long" (computed as ca. 1.7 Å) to make **1** isolable under normal conditions.[5] A bond length of 1.67 Å was determined experimentally for persistent hexakis(3,5-di-*tert*-butylphenyl)ethane (**2**),[6] which is obviously more sterically crowded. This counterintuitive finding and apparent discrepancy was addressed and rationalized just recently by one of us showing that the attractive dispersion interactions (London forces) between the *t*-butyl groups outweigh the otherwise unfavorable interactions of the phenyl moieties.[7]

Phenylethane dissociation may be prevented by bridging[8] and molecules such as tetraphenylcyclobuta[*b*]naphthenes contain very long (≥1.7 Å) C–C bonds. Such bond elongations were attributed to ring strain, through-bond couplings, and steric repulsions between the aromatic substituents.[9] The notion of a steric effect and its influence on molecular structure was first formulated in the 1930s.[10] However, the nature of steric effects was deemed almost exclusively repulsive ("steric hindrance"), as emphasized in the current definition by the IUPAC: "*Steric effects arise from contributions ascribed to strain as the sum of (1) non-bonded repulsion, (2) bond angle strain, and (3) bond stretches and compressions*".[11] Here we will emphasize a view that also includes *attractive* steric interactions leading to structures with extraordinarily long bonds that are nevertheless thermally very stable.

The most obvious way to elongate a given C–C bond is to increase the steric repulsions around it. This, typically, leads to

Received: March 7, 2012
Published: July 26, 2012

   dx.doi.org/10.1021/ja302258q | *J. Am. Chem. Soc.* 2012, 134, 13641–13650

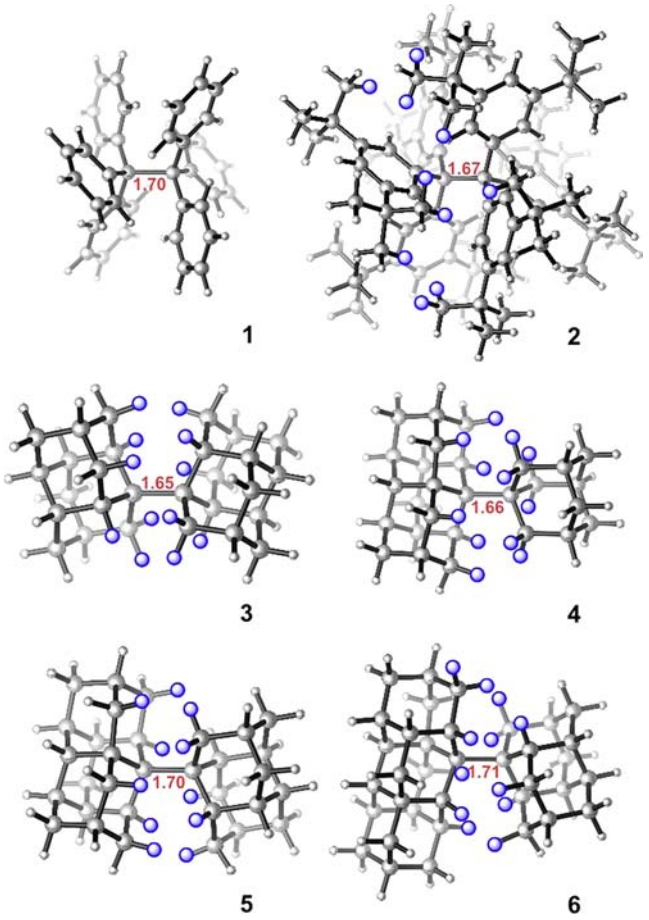

Figure 1. Sterically hindered arylethane derivatives (**1** and **2**) and crowded alkanes **3**–**6** that contain very long single C–C bonds. Selected hydrogens contributing to the dominant dispersion attractions around the central bonds are marked in blue.

elongations of neighboring bonds as well as to angular deformations. For instance, the bulky *tert*-butyl and 1-adamantyl groups cause C–C bond elongations (to 1.63–1.64 Å) of all neighboring C–C bonds in 2,3-di-tertbutyl-[12] and 2,3-di(1-adamantyl)-[13] derivatives of 2,3-dimethylbutane, which are stable at room temperature but decompose rapidly upon heating: the half-life of the adamantyl derivative at 167 °C is 1 h.[13b]

More crowded alkanes were predicted to be thermally unstable: for bond lengths larger than 1.70 Å, the estimated dissociation enthalpy already drops below 30 kcal mol^{-1}.[2,14]

We recently described the preparation of saturated hydrocarbons **3**–**5** that contain extremely long C–C bonds (1.65–1.70 Å).[15] These dimers are unexpectedly[2,14] thermally stable: differential scanning calorimetry showed that **3** melts without decomposition at 360 °C and **5** is stable upon heating up to 200 °C.[15] Because of the rigidity of the diamondoid[16] cages, the radicals formed through dissociation are structurally very similar to the hydrocarbon moieties in undissociated dimers. We suggested that the unusual stability of **3**–**5** arises from overall *attractive* dispersion interactions between the intramolecular CH···HC contact surfaces around the central C–C bond as shown in Figure 1. The role of such "dispersion energy donors"[17] is not limited to **3**–**5**, as the stability of more crowded **2** over **1** is determined by numerous dispersion attractions between CH···HC fragments of the *tert*-butyl groups.[7]

The rationalization of the role dispersion plays in constructing stable molecules with very unusual bonding situations leads the way to utilize dispersion as a design element for new materials,[18] but also extends to other areas of chemistry. The examination of such unusual structures as **3**–**5** also helps analyze the transition between the molecular and microscopic (i.e., material) level. In combination with the possibility of band gap tuning in sp^3-nanocarbon particles,[19] this provides numerous opportunities in designing new carbon materials.[20] This requires, however, more detailed information about such unusual bonding situations.

In the present paper, we describe the preparation of highly crowded cross-dimer of [121]tetramantane with diamantane (**6**), which sets a new alkane CC bond length record of 1.71 Å. In contrast to common expectations, alkanes with such long bonds can still be very stable (under ambient conditions) and we outline in the following the likely origins of this remarkable stability. We also present the fascinating dynamic behavior of diamondoid dimers **3**–**6** both experimentally and computationally, and we predict the existence of stable molecules with even longer C–C bonds.

Only recently it became possible to include dispersion interactions in DFT[21] allowing an assessment of their contributions to the stabilities of molecular structures. We employ DFT computations with dispersion included explicitly,[22] functionals that account for the medium-range correlations[23] as well as several other DFT and ab initio methods. As pointed out earlier, DFT methods have to be applied with caution for large systems as they show growing energy errors with increasing system size.[24] As the van der Waals (vdW) contributions are very large in **3**–**6**, the structural and energetic description of these molecules provide an ideal testing ground for new theoretical approaches.

RESULTS AND DISCUSSION

Preparation of Diamondoid Dimers. Diamondoids[16] of various sizes and topologies are readily available from crude oil[25] and their selective C–H bond functionalizations are now well established.[26] Wurtz coupling (Scheme 1) of the respective bromides[26c,27] in xylene under reflux gave the respective diamondoid dimers **3**–**9** in good preparative yields. Note that these dimers formally also are diamondoids because they present sections of a hydrogen-terminated diamond lattice. One obvious driving force behind this research is therefore the construction of diamond from diamondoids.[28]

As mixtures of different dimers form in cross-coupling reactions, the isolation and purification of heterodimers **4**–**7** required a number of sublimation and crystallization steps (see Experimental Section). Dimers **3**–**9** were fully characterized and all NMR resonances were assigned utilizing comparative analyses of COSY, HSQC, HMBC, and TOCSY spectra (see Supporting Information for details). Dimer **6**, whose structure was confirmed by X-ray analysis, contains a 1.71 Å central CC bond (Figure 2), the longest on record for an alkane. Remarkably, **6** is stable upon heating and the crystals melt only at 246 °C. Previous experience shows that there is a very clear linear correlation between the melting points of such structures (**3**–**5**) and their intrinsic stability as assessed from thermogravimetric and differential scanning calorimetric measurements in solution. Hence, there is a good correlation

dx.doi.org/10.1021/ja302258q | J. Am. Chem. Soc. 2012, 134, 13641–13650

Scheme 1. Preparation of Diamondoid Dimers (3–9)[a]

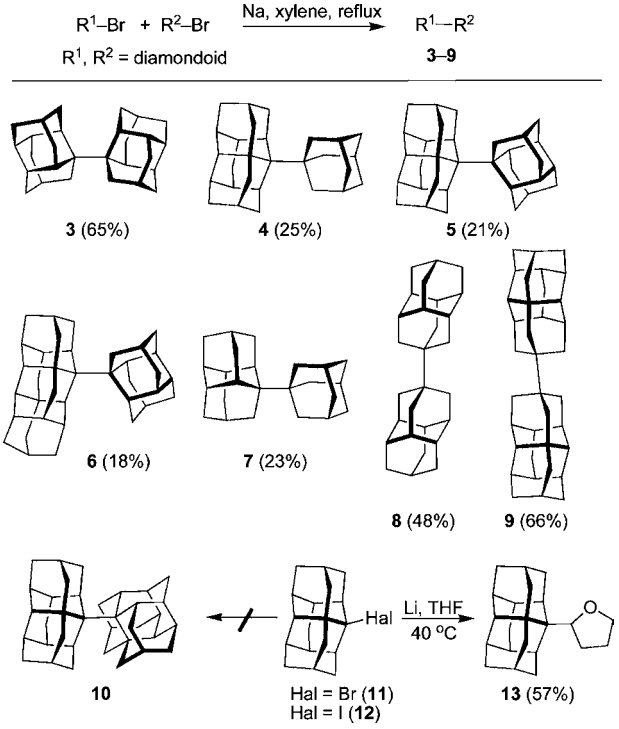

[a]Yields are given for pure compounds prepared at preparative scale.

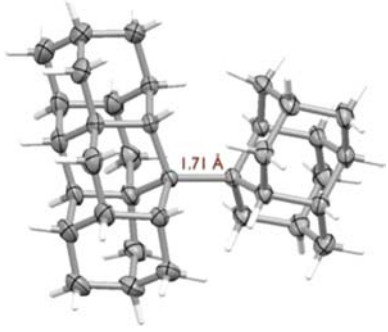

Figure 2. X-ray crystal structure of **6**; carbon atoms are shown with 50% probability ellipsoids (for crystal packing see Supporting Information).

between the thermal behavior of these compounds in the solid state and in solution.[15]

Our attempts to couple 2-bromotriamantane (**11**) as well as the 2-iodotriamantane (**12**) under milder conditions, at best led to the THF adduct (**13**) rather than to **10** (Scheme 1). Does this imply that **10** is over the limit for constructing very long C–C bonds stable at 40 °C?

Diamondoid Dimers as Theory Benchmarks. A computational assessment of the properties (e.g., rotational barriers, BDEs, heats of formation, etc.) of **3–9** as well as hypothetical **10** is challenging, as high end benchmark ab initio methods cannot be used owing to the sizes of the systems. We had already shown that the B3LYP approach is not able to reproduce the experimental X-ray geometries of **2**[7] as well as **3–5**[15] satisfactorily. For instance, the B3LYP/6-31G(d,p) computed central C–C bond length in **3** is 1.674 Å, which significantly exceeds the experimental value of 1.647 Å. Reoptimization with inclusion of a posteriori dispersion corrections (B3LYP-D[22a]) shortens the bond to 1.653 Å, clearly demonstrating the importance of dispersions for the structure of **3**.[15]

To find the most adequate computational approach, we first examined the ability of various DFT functionals to reproduce the experimental geometry and the rotational barrier in **3** as a model. We employed several DFT and ab initio methods utilizing both Pople's 6-31G(d,p) as well as Dunning's correlation-consistent cc-pVDZ[29] basis set. From the X-ray crystal structure data[15] **3** adopts a C_2-symmetric *gauche* conformation with a central CC bond length of 1.647 Å. While different basis sets alter the geometry only slightly, the deviations observed for the various methods are large. The largest deviations from the experimental value were found for BLYP,[30] B3LYP,[31] and B98[32] (Figure 3, left part). Incorporation of empirical London dispersion corrections[21] through the DFT-Dn[22a,33] approaches shortens the central CC bond to ca. 1.65 Å, which is close to experiment. Good agreement with experiment was also found for functionals that either account for long-range correlations in combination with the DFT-D scheme (wB97XD[34]) or utilize an improved gradient non-locality correction[35] such as PBE1PBE;[36] PBE type functionals are known to account better for medium range correlation effects than BLYP or B3LYP.[24c] Notably, the inclusion of long-range corrections based on exchange only without accounting for dispersion (LC-BLYP)[37] underestimates the bond length by 0.02 Å; M06-2X shows close agreement with the X-ray geometry.[38] Perfect agreement between the computed and measured (by X-ray crystal structure analysis) is not possible without correcting for zero-point vibrations and other effects. However, these changes are expected to be at most in the range of a few tenths of an angstrom but are typically much smaller. Furthermore, the CC bonds of hydrocarbons in the solid state usually are shorter relative to those in the gas phase. For instance, the CC bond length of 1.532 Å found for solid ethane[39] is shorter than that determined in the gas phase by electron diffraction (1.534 Å)[40] or infrared spectroscopy (1.535 Å).[41] The same situation holds for cyclohexane where all CC bonds in the crystal X-ray diffraction experiment (1.523 Å)[42] are shorter than those from electron diffraction (1.535 Å);[43] for 2,2,3,3-tetramethylbutane, the central CC bond length is 1.573 Å[44] in the crystal versus 1.582 Å in the gas phase.[45] Taking these deviations as empirical corrections, we estimate that a value of 1.655 Å would be the most realistic approximation of

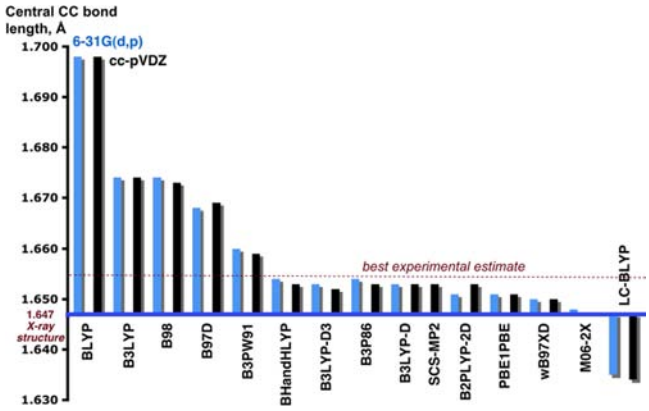

Figure 3. Computed central C–C bond lengths of the most stable conformer of **3** at various levels of theory.

dx.doi.org/10.1021/ja302258q | J. Am. Chem. Soc. 2012, 134, 13641–13650

the central bond length for **3** in the gas phase. This is in excellent agreement with the most trusted ab initio SCS-MP2/cc-pVDZ[46] optimization that gives a value of 1.653 Å. The B3LYP-Dn and PBE1PBE functionals describe the geometry of **3** well while the M06-2X and wB97XD methods underestimate the central CC bond length slightly (Figure 3). We also tested the ability of the above functionals to reproduce the geometries of **5**[15] and **6**. We optimized the most stable conformer of **5** with several DFT/6-31G(d,p) methods and found very good agreement with the experiment for B3PW91 (1.707 Å), B97D (1.718 Å), B3LYP-D (1.698 Å). Other approaches fail: 1.729 Å at B3LYP, 1.765 Å at BLYP, and 1.725 Å at B98. The same is true for **6** where the best agreement with the experimental geometry was found at B97D (1.721 Å) and B3PW91 (1.714 Å).

However, as we pointed out earlier, even the "good" DFT geometries do not necessarily indicate a proper energetic description when dealing with large hydrocarbon molecules.[24b] To probe this, we modeled the full rotational potential for the interconversion of the two enantiomeric *gauche* conformers at the above DFT levels of theory and compare these with the experimental value obtained through variable temperature NMR studies. As the inward (*endo*) CH terminated surfaces around the central C−C bond of **3** are not perfectly parallel, some conformations are highly unfavorable leading to high rotational barriers. At the time scale of a 150 MHz ^{13}C NMR experiment, no dynamic behavior was observed for **3** at 298 K, as there are 14 signals in the spectrum (Figure 4). The signals

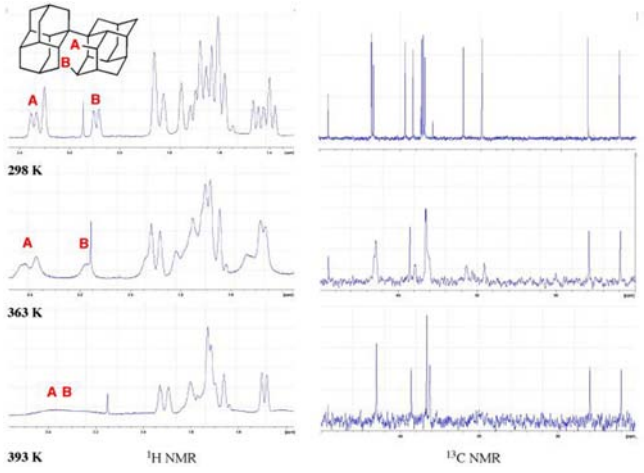

Figure 4. ^{1}H- and ^{13}C NMR spectra of **3** at various temperatures.

of the *endo*-protons H_A and H_B are well resolved in the 600 MHz ^{1}H NMR spectrum at room temperature. However, even moderate heating causes major changes where, owing to the acceleration of the exchange, the H_A and H_B resonances coalesce at 363 K with corresponding changes observed in the ^{13}C NMR spectrum (Figure 4). The experimental activation enthalpy for partial (vide infra) rotation around the central CC-bond in **3** was determined by line shape analysis for the signal at 28.7 ppm in the ^{13}C NMR at eight different temperatures (Figure S17). This gives an experimental value for $\Delta H_{298}^{\ddagger}$ = 16.0 ± 1.3 kcal mol^{-1}.

Although M06-2X did very well in reproducing the minimum ground state geometry, it apparently does not do so well for this rotational transition structure as it overestimates the experimental barriers by more than 3 kcal mol^{-1} (Figure 5).

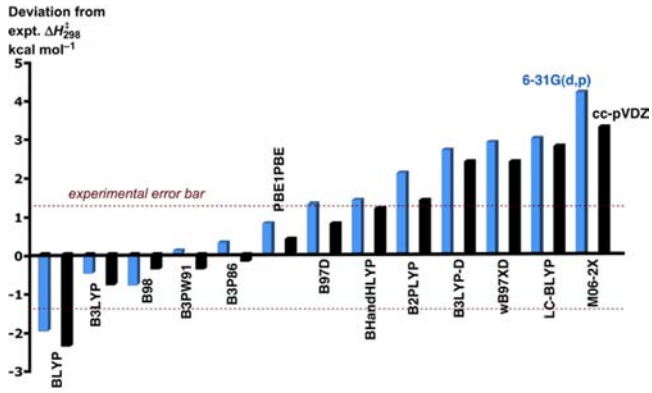

Figure 5. Absolute deviations from the experimental rotational barrier (16.0 ± 1.3 kcal mol^{-1}, determined by variable temperature NMR) for **3** computed at various levels of theory.

The LC-BLYP and dispersion corrected DFT functionals overestimate the barrier by 1−3 kcal mol^{-1}. In contrast, BLYP underestimates the barrier by ca. 2 kcal mol^{-1}. In general, common DFT functionals such as B3LYP, B98, B3PW91,[36] B3P86,[47] PBE1PBE, BHandHLYP[48] are able to reproduce the rotational barrier within the experimental uncertainty (16.0 ± 1.3 kcal mol^{-1}) presumably due to error cancellations. Note that the PBE1PBE and B3P86 methods reproduce the geometry of **3** well and at the same time satisfactorily reproduce the barrier, but the best overall agreement was found for B3PW91. This is in line with the earlier observation of the ability of the PW91 functional to account partially for medium-range dispersion interactions;[49] this is particularly important for the smaller systems **3** and **7**; systematic studies are needed for the larger systems to determine the effect of long-range dispersion corrections neglected with this approach. B3PW91 also reproduces well the isomer energy differences of many hydrocarbons.[24b] Solvent effects have only little influence on the rotational exchange since SCRF computations utilizing the PCM model[50] gave essentially the same barrier heights as the gas phase computations (16.0 kcal mol^{-1} at B3PW91/6-31G(d,p)).

On the basis of our benchmarking of various DFT methods utilizing the experimental geometry and the rotational barrier of **3**, we choose the B3PW91/6-31G(d,p) approach for the computations of other diamondoid dimers. Extension of the basis set does not change this picture (we computed a 16.1 kcal mol^{-1} rotational barrier for **3** at B3PW91/6-311+G(d,p)). However, since the DFT computations may be sensitive to molecular size we compare our B3PW91/6-31G(d,p) results with B3LYP-D and M06−2X computations.

The stationary structures on the potential energy hypersurface (PES) for the rotation around the central CC bond of **3** are determined by the direction of the rotation (Figure 6) and include three transition structures and three minima. The barrier for the *concerted* enantiomerization of **3a** is very high (33.0 kcal mol^{-1}) due to unfavorable repulsions of the *endo*-hydrogens in the C_{2v} symmetric **TS1** (Figure 6). The alternative stepwise rotation through **TS2** and **TS3** and the *gauche* enantiomeric intermediates **3b** requires the 16.0 kcal mol^{-1} barrier (16.0 ± 1.3 kcal mol^{-1} from the experimental NMR data, vide supra).

Dynamic Behavior of 4−7. Hydrocarbons **4**−**7** demonstrate even more fascinating dynamic behavior than **3**. Two nondegenerate, almost isoenergetic paths exist for the

dx.doi.org/10.1021/ja302258q | J. Am. Chem. Soc. 2012, 134, 13641−13650

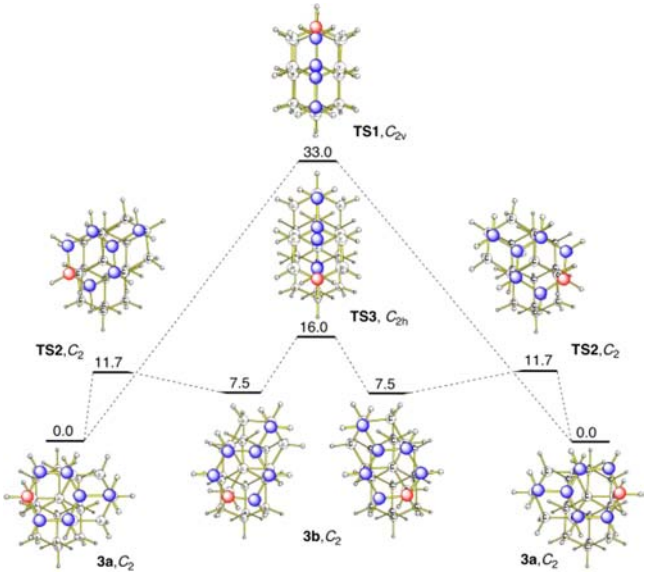

Figure 6. B3PW91/6-31G(d,p) computed barriers ($\Delta H^{\ddagger}_{298}$, kcal mol^{-1}) for the rotation around the central CC bond of **3**. The blue and red colored carbon atoms are used as visual aids to follow the rotational motions.

interconversion of chiral conformer **4a**, which is the energy minimum for **4** (Figure 7). This represents the unusual

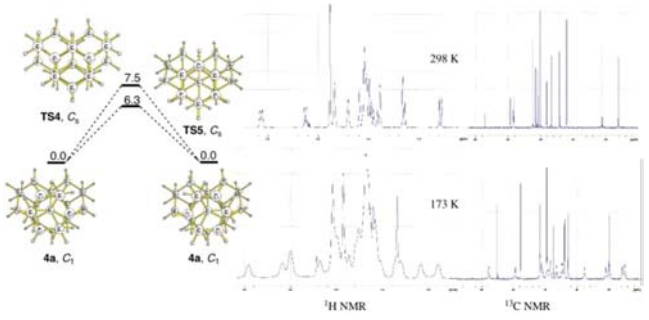

Figure 7. B3PW91/6-31G(d,p) computed barriers (ΔH_{298}, kcal mol^{-1}) for the rotation around the C−C bond of **4** and the ^{1}H- and ^{13}C NMR spectra measured at different temperatures.

situation that both eclipsed **TS4** and staggered **TS5** have similar energies (ca. 6−7 kcal mol^{-1}). Hence, while we had to heat **3** to determine the rotational dynamics, only lowering the temperature reveals the rotational dynamics of **4**! At 173 K, the lowering of the rate of exchange between **4a** gives NMR spectra attributed to the C_1 structure (Figure 7); however, we were not able to determine the exchange completely at that temperature due to the relatively low rotational barriers.

The potential around the C−C-bond of **5** involves three C_1 conformers **5a**−**5c** (Figure 8). Conformers **5b** and **5c** are substantially less stable than **5a**, which is likely to be the only one populated. The enantiomerization of **5a** through **TS6** requires 7.7 kcal mol^{-1} barrier and we are able to "freeze" this conformer at 200 K. At that temperature, the ^{13}C NMR spectrum, which contains 32 different carbon resonances, is in complete agreement with the C_1-point group of **5a**. The full rotation around the central C−C bond requires passing through two high-energy transition structures **TS7** and **TS8**. The rotational potential of **6** contains six C_1-minima with the two most stable (**6a** and **6b**) shown in Figure 9 (for the full

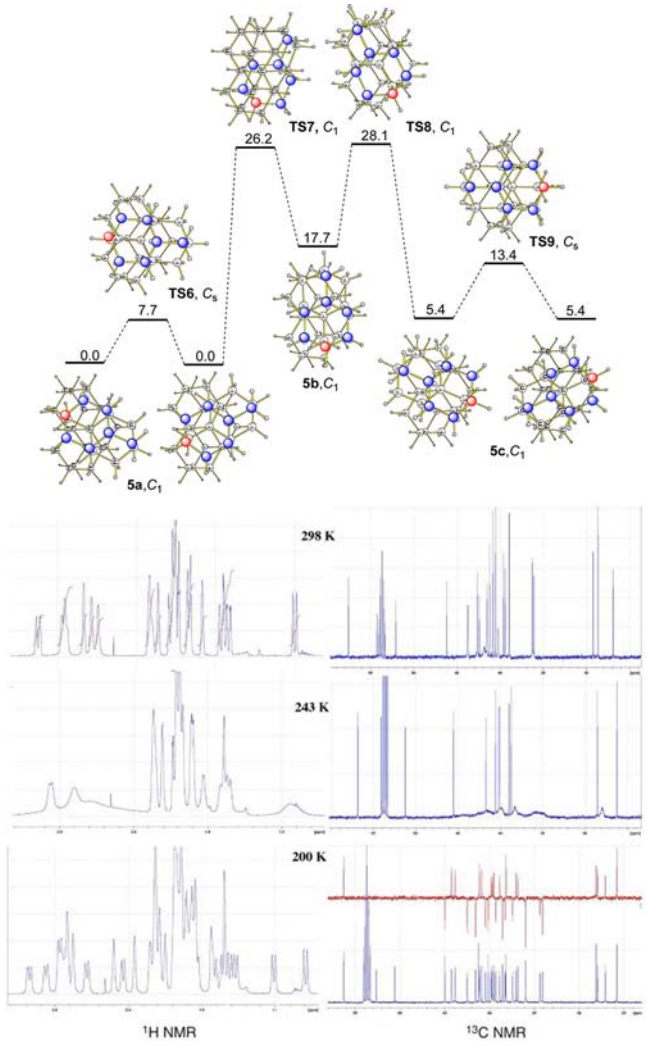

Figure 8. B3PW91/6-31G(d,p) computed barriers (ΔH_{298}, kcal mol^{-1}) for the rotation around the C−C bond of **5** and the NMR spectra measured at different temperatures.

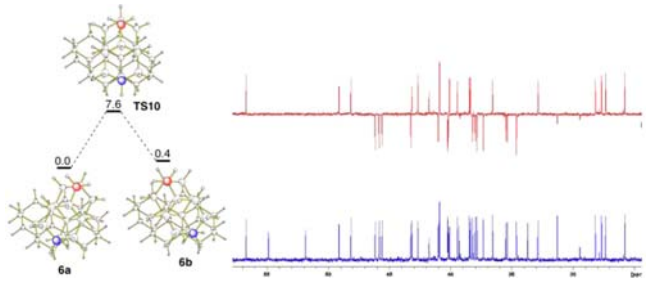

Figure 9. Interconversion of the two most stable conformers (B3PW91/6-31G(d,p) ΔH_{298}, kcal mol^{-1}) of **6** and its ^{13}C and DEPT NMR spectra measured at 333 K.

picture see Supporting Information). These two minima energetically lie within 0.1−0.7 kcal mol^{-1} in favor of **6a** at all levels of theory employed (B97D, B3PW91 and B3LYP-D). Yet, less stable **6b** was found in the crystal structure (cf. Figure 2) presumably due to better packing (see SI). Conformers **6a** and **6b** interconvert with the barrier of 7.6 kcal mol^{-1} (at B3PW91) through **TS10**. The ^{13}C NMR spectrum measured at 333 K contains 14 CH_2, 18 CH, and 4 C resonances (Figure 9) attributed to the averaged C_1-structure of **6**.

dx.doi.org/10.1021/ja302258q | J. Am. Chem. Soc. 2012, 134, 13641−13650

Dimer **7** adopts a chiral C_1 *gauche*[51] conformation (**7a**) but the enantiomerization through staggered **TS11** has a very low barrier ($\Delta H_{298}^{\ddagger}$ = 1 kcal mol^{-1}, Figure 10). This results in the

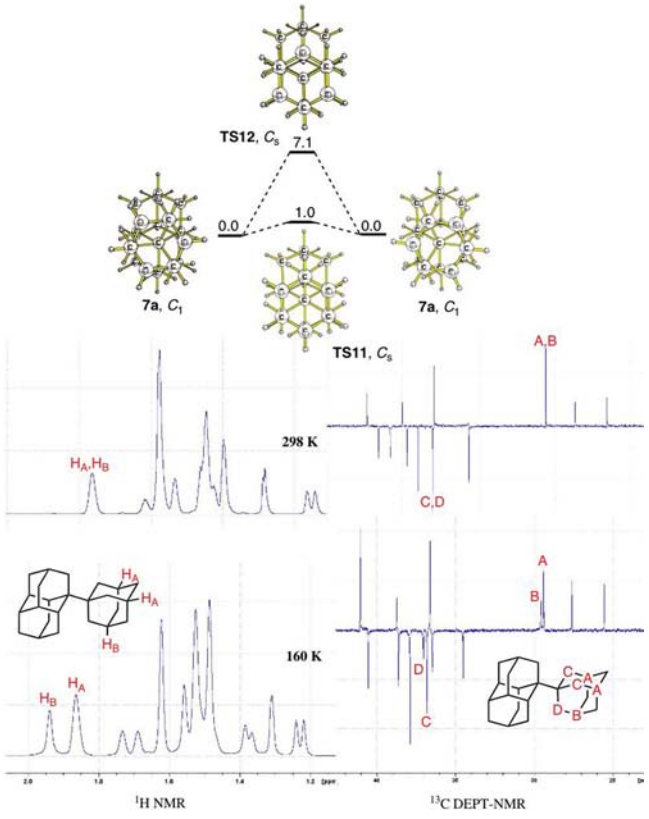

Figure 10. B3PW91/6-31G(d,p) computed barriers (ΔH_{298}, kcal mol^{-1}) for the partial (**TS11**, enantiomerization) and full (**TS12**) rotation around the central C−C bond of **7** and the NMR spectra measured at different temperatures.

averaging of the NMR resonances of the adamantyl AB and CD fragments at room temperature. The computed barrier for the full rotation around the C−C bond through eclipsed **TS12** is much higher ($\Delta H_{298}^{\ddagger}$ = 7.1 kcal mol^{-1}) and lowering the temperature to 160 K allows the observation of an effective C_s-symmetric structure resulting from fast averaging of two enantiomeric C_1 forms of **7a** trough **TS11**. As a consequence, the ^{1}H NMR spectrum measured at 160 K displays different signals for the tertiary H_A and H_B protons of the C_s symmetrical adamantyl fragment. The ^{13}C NMR spectrum at 160 K consists of 14 carbon resonances for which the nonequivalent adamantyl carbons A, B, C, and D were assigned based on the DEPT spectrum (Figure 10, and Supporting Information for further assignments).

Note that the IUPAC rule defines a rotational barrier as "*...the potential energy barrier between two adjacent minima...*",[52] so one must make a clear distinction whether a full or a partial rotation is described. Otherwise, one could say that **7** has a *lower* rotational barrier than ethane. This does not make sense, and it renders the current IUPAC definition as arbitrary. We suggest that a rotational barrier should rather be referred to as "*the energy required for a full rotation around a bond.*"

Importantly, the PESs obtained for **3**−**7** at the B3PW91 lever differs only slightly (<10%) from those obtained with the B3LYP-D and M06−2X functionals. We conclude that the dynamic behavior of **3**−**7** is determined by the shape of the inward CH surfaces that surround the central C−C bond. Although these bonds connect topologically related moieties, the computed rotational barriers vary dramatically (from ca. 7 kcal mol^{-1} in **7** to 33 kcal mol^{-1} in **3**).[53] Thus, the shapes and contact areas of the interacting CH surfaces rather than the central C−C bond lengths determine the barriers. We conclude that the DFT computations satisfactorily reflect the dynamic behavior of **3**−**7** effectively reproducing the rotational potentials.

Strain Energies. We computed the strain energies (Figure 11) through homodesmotic equations[54] utilizing unstrained

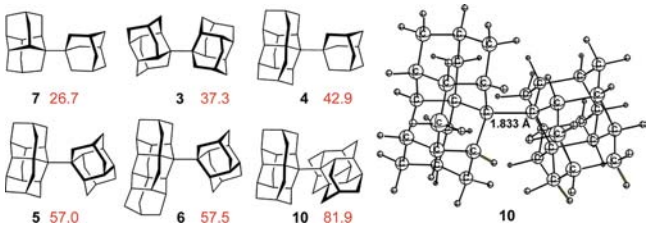

Figure 11. Computed strain energies (B3PW91/6-31G(d,p), kcal mol^{-1} in red) of hydrocarbon dimers and the optimized geometry of hypothetical triamantane dimer **10**.

reference hydrocarbons (ethane, isobutane, and neopentane) in analogy to our previous studies on large-ring propellanes[55] and diamondoids.[26a] The strain energy of parent 1-(1-adamantyl)-adamantane) whose central bond is lengthened only slightly (1.578 Å from the X-ray crystal structure analysis,[56] and 1.586 Å computed at B3PW91/6-31G(d,p)) is only 12.7 kcal mol^{-1}, which is comparable to the strain energy of two individual adamantane molecules (ca. 6 kcal mol^{-1} each).[57] In the series of dimers the bond lengths and strain energies are indirectly proportional due to the growing number of unfavorable (i.e., shorter than ideal vdW contact of 2.2 Å[58]) H···H distances. Dimer **10** is the most strained and has a remarkable long central C−C bond of 1.833 Å at B3PW91 (1.847 Å at B97D). It is a minimum on the PES and represents a formidable but realistic synthetic challenge since its computed BDE is large and positive (+36.1 kcal mol^{-1}).

Large Diamondoid Clusters. The generalization of our findings may reveal important details about the bonding situations between H-terminated surfaces with many CH···HC contacts. In contrast to triamantane, perfectly planar hydrogen-terminated {111}-surfaces are present in the larger diamondoids T_d-pentamantane[25b,26b] and cyclohexamantane,[25c,26h] which may also be viewed as double-layered [13]graphane.[18] Such diamondoids with many parallel C−H bonds on their surfaces, may potentially offer immense possibilities for the construction of hydrocarbons with very long C−C distances (and possibly even with unpaired electrons). Because of the additivity of the vdW attractions,[59] the energetic gains may be even larger than from covalent bonding. To probe this idea, we also computed the interaction energies of much larger diamondoids to show that additive dispersion interactions may quickly override the covalent contribution. We demonstrated recently utilizing the B97D and M06-2X methods that the association energies for graphane vdW complexes reach 120 kcal mol^{-1} already at 2 nm particle size ([97]graphane dimer).[18] As a result, graphanes adopt multilayered structures[18,60] similar to graphenes. We found that B97D satisfactorily reproduces the intermolecular vdW contact distances found in the elementary cells of diamondoids from

dx.doi.org/10.1021/ja302258q | J. Am. Chem. Soc. 2012, 134, 13641−13650

X-ray crystal diffraction analysis, in contrast to M06−2X, which somewhat underestimates these distances.[61] We computed a continuous increase in the B97-D3/6-31G(d,p)//B97D/6-31G(d,p) dimerization exothermicites from adamantane (−4.3 kcal mol^{-1}) to diamantane (−6.4 kcal mol^{-1}), and triamantane (−10.2 kcal mol^{-1}). At a certain stage of enlargement, the bonding energy of two hydrocarbon radicals must be determined by dispersion interactions only. For instance, large hydrocarbon $C_{82}H_{76}$ (**14**) forms a stable vdW dimer $C_{164}H_{152}$ (**15**) with a dissociation energy of +43.7 kcal mol^{-1} (Figure 12). As a consequence, the dimerization of two

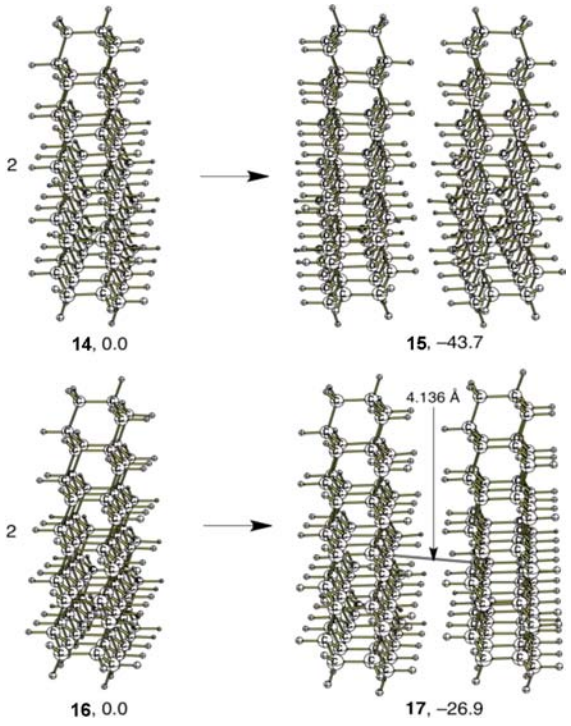

Figure 12. B97-D3/6-31G(d,p)//B97D/6-31G(d,p) binding energies of vdW complexes **15** and **17** formed from the dimerization of two neutral diamondoids **14** and two diamondoid radicals **16**, respectively.

alkyl radicals $C_{82}H_{75}$· (**16**) derived from **14** gives $C_{164}H_{150}$ structure **17** with an association energy of −26.9 kcal mol^{-1}, implying that **17** should be stable under mild conditions despite the fact that it *formally* contains a superlong (ca. 4 Å) "CC bond" between the radical centers, representing the extreme case of bond stretching. One should not claim the presence of the C−C bond in such structures; however, the situation in **17** is clearly different from that in bulky alkyl radicals, e.g., *tert*Bu_3C·, where intermolecular association is prevented by much fewer H···H-contacts and the flexibility of the molecule. Clearly, the association between the planar and rigid hydrogen-terminated surfaces determine the stability of **17**. This is also in marked contrast to derivatives that display large distance between formally configurationally unsaturated carbon atoms but whose long bond stability is determined by "external" covalent bridging.

Our experimental proof-of-principle that attractive dispersion interactions may create unusual bonding situations where, for instance, the dimer and the respective alkyl open-shell states are comparable in energies opens new avenues in the construction of novel materials. Many natural and synthetic bulk materials possess large CH surfaces and their properties are determined by vdW forces. This may be the case for diamond films or diamond(oid)-modified metal surfaces that are closely related in electronic properties as we have shown recently,[62] and graphanes, whose multilayered structure was recently predicted.[18,60a,63] H···H-dispersion attractions are also likely to be responsible for the strong conglomerations of nanodiamond materials.[64]

These findings may change the common view that sp^3 carbon materials have only limited applications in electronics due to strong confinement of spin/hole states.[65] While this is true for **16**, its double-layered form **17** is likely to show pronounced electron mobility, and that such structures are worthwhile targets that may be useful for the construction of new organic spintronic materials.[20,66] This, in addition to conventional band gap tuning[19] opens numerous opportunities in designing new high spin and hole-transport carbon materials and even superconductors.[60b] The presence of electron holes on the surface of radical-activated hydrogen-terminated diamond offers a viable explanation for its conductivity.[67]

■ CONCLUSIONS

We synthesized diamondoid dimers **3**−**6** that display extraordinarily long central C−C bonds. Structure **6** displays the longest C−C bond (1.71 Å from the X-ray crystal structure analysis) observed to date in an alkane. Empirical bond length-bond strength correlations that predict the instability of the molecules with such a long C−C bonds do not hold because **3**−**6** are very stable even at elevated (well above 200 °C) temperatures. The unusual stability of **3**−**6** is likely to arise from numerous attractive dispersion attractions between inward H-terminated surfaces surrounding the long bonds. As these surfaces are not perfectly parallel, the rotational barriers vary significantly as determined by variable temperature NMR spectroscopy.

Utilizing diamantane dimer **3** as a model compound, we probed the ability of various DFT methods to reproduce the experimental X-ray crystal structure geometry and the measured rotational barriers. Not unexpectedly, inclusion of dispersion corrections is essential for an accurate description of the geometries. The computation of the rotational barriers is less critical as many common DFT functionals were able to reproduce these due to fortuitous error cancellation.

While less sterically encumbered 9-(9-triamantyl)-triamantane (**9**) could readily be prepared, the unsuccessful attempts to prepare the more hindered side-on dimer **10** seem to indicate the limit of our ability to prepare even more sterically encumbered compounds with even longer central C−C bonds. However, further expansion of the H···H contact areas may lead to the formation of stable hydrocarbon assemblies with binding energies comparable or even exceeding those of typical C−C single bonds.

■ COMPUTATIONAL METHODS

All structures were fully optimized utilizing the Gaussian09 program suite.[68] B3LYP-D3 computations were performed with Gamess 11.1.[69] The DFT-D2 and SCS-MP2 optimizations were performed with ORCA 2.8.0.[70] Second derivatives were computed analytically to confirm that all structures are either minima (NIMAG = 0) or transition structures (NIMAG = 1).

■ EXPERIMENTAL SECTION

2-(1-Diamantyl)[121]tetramantane (6). 1-Bromodiamantane (1.07 g, 4 mmol) and 2-bromo-[121]tetramantane (0.47 g, 1.3

dx.doi.org/10.1021/ja302258q | J. Am. Chem. Soc. 2012, 134, 13641−13650

mmol)[26c] were dissolved in 1.5 mL of dry *m*-xylene and refluxed (140−150 °C in the oil bath) in a two-neck flask fitted with an argon inlet, and an anchor stirrer with an air-cooled condenser under a slow stream of argon. A total amount of 0.23 g (10 mmol) of small pieces of sodium was added to the stirred reaction mixture over 2 h. After addition of all sodium, the mixture was refluxed for a total of 4 h, cooled to 40 °C, and the excess of sodium was quenched with methanol. After cooling to room temperature, the reaction mixture was filtered and washed with water, evaporated, and separated on silica gel (*n*-hexane) to give a mixture of hydrocarbons; the mixture of diamantane and tetramantane was sublimed off at 130 °C/0.2 mmHg, and, additionally at 150 °C/0.05 mmHg. Crystallization of the residue from hexane gave **3** and a mother liquor enriched with **6**. Triple crystallization of mother liquor from hexane gave 109 mg (18%) of hydrocarbon **6** as colorless crystals mp = 246−247 °C (dec). ^{1}H NMR spectrum (600 MHz, 298 K, $CDCl_3$, δ, ppm): 2.66 − 2.60 d (J = 12 Hz, 1 H), 2.57 s (1 H), 2.55−2.49 d (J = 12 Hz, 1 H), 2.48−2.44 d (J = 12 Hz, 1 H), 2.43−2.31 m (5 H), 2.22−2.16 m (2 H), 1.94 bs (1 H), 1.9 bs (3 H), 1.84 bs (3 H), 1.8 bs (1 H), 1.77−1.67 m (8 H), 1.66−1.59 m (7 H), 1.54 s (1 H), 1.47−1.39 m (2 H), 1.38−1.26 m (6 H), 1.23−1.17 d (J = 12 Hz, 1 H), 1.07−1.03 d (J = 12 Hz, 1 H), 0.92−0.85 d (J = 12 Hz, 1 H). ^{13}C NMR spectrum (150 MHz, 298 K, $CDCl_3$, δ, ppm): 56.7 (CH), 54.9 (C), 51.8 (C), 49.2 (CH), 48.2 (CH), 46.1 (CH_2), 45.9 (CH_2), 45.6 (CH_2), 43.3 (CH_2), 43.2 (CH), 42.7 (CH), 41.8 (CH), 41.0 (CH_2), 40.9 (CH), 40.9 (CH) 40.3 (CH_2), 40.1 (CH), 39.5 (CH), 39.3 (C), 38.5 (CH), 38.4 (CH), 38.2 (CH_2), 38.0 (CH_2), 37.9 (CH_2), 37.4 (CH_2), 36.5 (CH), 35.5 (CH_2), 35.4 (CH_2), 34.7 (CH_2), 33.7 (C), 33.0 (CH), 31.3 (CH_2), 28.1 (CH), 27.6 (CH), 27.3 (CH), 25.8 (CH). MS (m/z > 10%): 292, 291, 188, 187, 149, 120, 98, 91, 83, 55 (100%). HR−MS (m/z): found for ($C_{22}H_{27}$ + $C_{14}H_{19}$) (291.2112 + 187.1486); calcd for ($C_{22}H_{27}$ + $C_{14}H_{19}$) (291.2113 + 187.1487).

1-(1-Adamantyl)diamantane (7). 1-Bromoadamantane (0.4 g, 1.87 mmol) and 1-bromodiamantane (1.5 g, 5.6 mmol) were dissolved in 6 mL of dry *m*-xylene and refluxed (140−150 °C in an oil bath) as above. Sodium (0.8 g, 34.8 mmol) was added as small pieces to the stirred reaction mixture over 1 h. After all the sodium had been added, the mixture was refluxed for an additional 4 h, cooled to 50 °C, and the excess sodium was quenched with methanol. After cooling to room temperature the reaction mixture was filtered and washed with water, the solvents evaporated, and the mixture separated on silica gel (*n*-hexane) to give a mixture of hydrocarbons, which was crystallized from *n*-hexane. The mother liquor was evaporated, the mixtures of adamantane and diamantane were sublimed off at 80 °C/2 mmHg, and the residue was recrystallized twice from *n*-hexane to give 138 mg (23%) of **7** as colorless crystals mp = 316 °C. ^{1}H NMR spectrum (600 MHz, 298 K, $CDCl_3$, δ, ppm): 2.52 bd (J = 12 Hz, 2 H), 1.97 bs (3 H), 1.85−1.73 m (12 H), 1.67−1.63 m (9 H), 1.62−1.58 m (4 H), 1.53−1.5 m (2 H), 1.36 bd (J = 12 Hz, 2 H). ^{13}C NMR spectrum (150 MHz, 298 K, $CDCl_3$, δ, ppm): 41.6, 41.2, 40.8, 40.4, 40.2, 39.3, 39.2, 38.2, 37.4, 37.3, 35.0, 29.7, 27.8, 25.7. MS (M/Z > 10%): 91, 105, 135, 187 (100%), 201, 270, 322. HR-MS (m/z): found 322.266, calcd for $C_{24}H_{34}$ 322.266; calcd. C, 89.37; H, 10.63; found C 89.48, H 10.47.

4-(4-Diamantyl)diamantane (8). 4-Bromodiamantane (2.88 g, 11 mmol) was dissolved in 12 mL of dry *m*-xylene and heated to reflux in a two-neck flask fitted with an argon inlet, anchor stirrer with air-cooled condenser under a slow stream of argon. Sodium (0.3 g, 13 mmol) was added in small pieces to the stirred reaction mixture over 1 h. After all sodium had been added, the mixture was refluxed for additional 4 h, cooled to 50 °C, and excess sodium was quenched with methanol. After cooling to room temperature, the reaction mixture was filtered and washed with water, evaporated and separated on silica gel (*n*-hexane) to give a mixture of hydrocarbons, which was crystallized from benzene to give 0.97 g (48%) of colorless crystals of **8**, mp = 360 °C (dec). ^{1}H NMR spectrum, δ, ppm: 1.75−1.7 m (8 H), 1.67−1.65 m (12 H), 1.57 bs (6 H), 1.46−1.51 m (12 H). ^{13}C NMR spectrum (150 MHz, 298 K, $CDCl_3$, δ, ppm): 38.7, 38.3, 37.7, 36.7, 33.9, 26.3. MS (m/z): 186 (53%), 187 (100%), 188 (27%), 374 (16%). HR-MS (m/z): found 374.294, calcd for $C_{28}H_{38}$ 374.297.

9-(9-Triamantyl)triamantane (9). 9-Bromotriamantane (0.527 g, 1.65 mmol) was dissolved in 2.5 mL of dry *m*-xylene and heated to reflux in a two-neck flask fitted with argon inlet, anchor stirrer with air-cooled condenser under a slow stream of argon. Sodium (0.05 g, 2.17 mmol) was added in small pieces to the stirred reaction mixture over 1 h. After all sodium had been added, the mixture was refluxed for an additional 4 h, cooled to 50 °C, and excess sodium was quenched with methanol. After cooling to room temperature, the reaction mixture was filtered and washed with water, evaporated and separated on silica gel (*n*-hexane) to give a mixture of hydrocarbons, which was crystallized from *n*-hexane to give 260 mg (66%) of colorless crystals of **9**, mp = 344 °C (dec). ^{1}H NMR spectrum, δ, ppm: 1.83−1.78 m (2 H), 1.72−1.57 m (22 H), 1.53−1.44 m (10 H), 1.29 s (4 H), 1.22 d (J = 4 Hz, 4 H), 1.40 s (4 H). ^{13}C NMR spectrum (150 MHz, 298 K, $CDCl_3$, δ, ppm): 47.0, 46.2, 43.8, 39.3, 38.8, 38.7, 38.3, 36.4, 36.0, 35.6, 35.5, 34.0, 28.5.

2-Iodotriamantane (12). A mixture of 1.05 g (4.1 mmol) of 2-hydroxytriamantane[26c] and 8.3 mL of a 48% aqueous solution of hydroiodic acid was added and vigorously stirred for 12 h at room temperature. The reaction mixture was diluted with 15 mL of water, extracted with CH_2Cl_2 (3 × 10 mL) and the combined extracts were washed with Na_2CO_3 and Na_2SO_3 solutions, water and dried over Na_2SO_4. Evaporation gave 1.34 g of 2-iodotriamantane (89%). ^{1}H NMR spectrum (600 MHz, 298 K, $CDCl_3$, δ, ppm): 2.74 d (J = 14 Hz, 2 H), 2.46 s (2 H), 2.17 s (1 H), 1.86−1.6 m (16 H), 1.24 d (J = 14 Hz, 2 H). ^{13}C NMR spectrum (150 MHz, 298 K, $CDCl_3$, δ, ppm): 50.9, 50.5, 43.7, 41.3, 39.7, 38.9, 38.6, 37.9, 27.7. MS (m/z): 55, 67, 77, 91 (100%), 105, 128, 239. Found C, 59.23; H, 6.54, calcd for $C_{18}H_{23}I$ C, 59.02; H, 6.33

2-Triamantantyl-tetrahydrofuran (13). 2-Iodotriamantane (**12**, 0.73 g, 2 mmol) was dissolved in 6 mL of dry tetrahydrofurane and a total amount of 0.06 g (2.5 mmol) of small pieces of Li/Na alloy (5% Na) was added to the stirred reaction mixture over 3 h at 40 °C. After all alloy had been added, the mixture was stirred for additional 4 h, cooled, and the excess reagent was quenched with methanol, the reaction mixture was evaporated in vacuum, and separated on silica gel (*n*-hexane) to give 0.2 g triamantane. By changing the eluant to *n*-hexane/ether 10:1, 350 mg (57%) of ether **13** as colorless crystals mp = 104−105 °C (hexane) was obtained. ^{1}H NMR spectrum (600 MHz, 298 K, $CDCl_3$, δ, ppm): 4.6 m (1 H), 3.8 m (1 H), 3.67 m (1 H), 2.65 d (J = 12 Hz, 1 H), 2.4 d (J = Hz, 1 H), 2.01 d (J = 2 Hz, 1 H), 2.1 d (J = 12 Hz, 1 H), 1.85 s (1 H), 1.83−1.77 m (4 H), 1.77−1.59 m (12 H), 1.5 s (1 H), 1.39−1.31 m (2 H), 1.23 d (J = 12 Hz, 1 H), 1.1 d (J = 12 Hz, 1 H), 0.9 d (J = 12 Hz, 1 H). ^{13}C NMR spectrum (150 MHz, 298 K, $CDCl_3$, δ, ppm): 82.6, 67.4, 50.5, 43.6, 41.0, 40.1, 40.0, 39.7, 39.3, 39.1, 39.0, 38.8, 38.6, 37.5, 37.0, 36.1, 34.1, 33.1, 28.0, 25.6, 25.2. MS (m/z): 129 (6%), 143 (7%), 239 (100%), 240 (19%). HR-MS (m/z): found 310.230, calcd for $C_{22}H_{30}O$ 310.229.

X-ray Structure Determination for 6. Crystals were obtained as described above. The X-ray crystallographic data were collected at 193 K on a STOE IPDS-diffractometer equipped with a low temperature system (Karlsruher Glastechnisches Werk). Mo Kα radiation (λ = 0.71069 Å) and a graphite monochromator was used. Cell parameters were refined by using up to 5000 reflections. A sphere of data was collected with the φ-oscillation mode (frame width 1.0°; number of frames 190; irradiation time/frame 12 min). No absorption correction was applied. The structure was solved by Direct Methods in SHELXS97, and refined by using full-matrix least-squares in SHELXL97.[71] All non-H atoms were treated anisotropically. All H-atoms could be found in the difference Fourier syntheses and were refined isotropically. The structure of **6** is triclinic and was solved in space group $P\bar{1}$; a total of 509 parameters were refined to R_1 = 4.5% (2032 reflections with $F_o > 4\ \sigma(F_o)$) and wR2 = 13.4% (all 5249 reflections). Refinement was done with F^2.

■ ASSOCIATED CONTENT

Ⓢ Supporting Information

includes the copies of ^{1}H- and ^{13}C NMR and 2D-NMR spectra of new compounds as well as xyz-coordinates of computed

species. This material is available free of charge via the Internet at http://pubs.acs.org.

AUTHOR INFORMATION

Corresponding Author

aaf@xtf.kpi.ua; prs@org.chemie.uni-giessen.de

Notes

The authors declare no competing financial interest.

ACKNOWLEDGMENTS

We dedicate this paper to the memory of colleague and teacher Alexander G. Yurchenko (Kiev Polytechnic Institute). We thank Dennis Gerbig for technical help with the D3-corrected computations. This work was supported by the Ministry of Science and Education of Ukraine, the Deutsche Forschungsgemeinschaft as well as the National Science Foundation of the USA (DFG-NSF Schr597/12-1), and in part by the Department of Energy, Office of Basic Energy Sciences, Division of Materials Science and Engineering, under contract DE-AC02-76SF00515.

REFERENCES

(1) Allen, F. H.; Kennard, O.; Watson, D. G.; Brammer, L.; Orpen, A. G.; Taylor, R. *J. Chem. Soc., Perkin Trans. 2* **1987**, S1.

(2) Zavitsas, A. A. *J. Phys. Chem. A* **2003**, *107*, 897.

(3) Kaupp, M.; Metz, B.; Stoll, H. *Angew. Chem., Int. Ed.* **2000**, *39*, 4607.

(4) Rüchardt, C.; Beckhaus, H. D. *Angew. Chem., Int. Ed. Engl.* **1980**, *19*, 429.

(5) Arkin, C. R.; Cowans, B.; Kahr, B. *Chem. Mater.* **1996**, *8*, 1500.

(6) Kahr, B.; van Engen, D.; Mislow, K. *J. Am. Chem. Soc.* **1986**, *108*, 8305.

(7) Grimme, S.; Schreiner, P. R. *Angew. Chem., Int. Ed.* **2011**, *50*, 12639.

(8) (a) Toda, F.; Tanaka, K.; Sano, I.; Isozaki, T. *Angew. Chem., Int. Ed. Engl.* **1994**, *33*, 1757. (b) Toda, F.; Tanaka, K.; Stein, Z.; Goldberg, I. *Acta Crystallogr.* **1996**, *C52*, 177. (c) Toda, F.; Tanaka, K.; Watanabe, M.; Tamura, K.; Miyahara, I.; Nakai, T.; Hirotsu, K. *J. Org. Chem.* **1999**, *64*, 3102. (d) Takeda, T.; Kawai, H.; Herges, R.; Mucke, E.; Sawai, Y.; Murakoshi, K.; Fujiwara, K.; Suzuki, T. *Tetrahedron Lett.* **2009**, *50*, 3693. (e) Kawai, H.; Takeda, T.; Fujiwara, K.; Wakeshima, M.; Hinatsu, Y.; Suzuki, T. *Chem.—Eur. J.* **2008**, *14*, 5780. (f) Kammermeier, S.; Jones, P. G.; Herges, R. *Angew. Chem., Int. Ed. Engl.* **1997**, *36*, 1757.

(9) (a) Bettinger, H. F.; Schleyer, P. v. R.; Schaefer, H. F., III. *Chem. Commun.* **1998**, 769. (b) Baldridge, K. K.; Kasahara, Y.; Ogawa, K.; Siegel, J. S.; Tanaka, K.; Toda, F. *J. Am. Chem. Soc.* **1998**, *120*, 6167.

(10) (a) Adams, R.; Yuan, H. C. *Chem. Rev.* **1933**, *12*, 261. (b) Westheimer, F. H. In *Steric Effects in Organic Chemistry*; Newman, M. S., Ed.; John Wiley and Sons: New York, 1956.

(11) Müller, P. *Pure Appl. Chem.* **1994**, *66*, 1077.

(12) Winiker, R.; Beckhaus, H. D.; Rüchardt, C. *Chem. Ber./Recl.* **1980**, *113*, 3456.

(13) (a) Flamm-ter Meer, M. A.; Beckhaus, H. D.; Rüchardt, C. *Thermochim. Acta* **1984**, *80*, 81. (b) Flamm-ter Meer, M. A.; Beckhaus, H. D.; Peters, K.; von Schnering, H. G.; Rüchardt, C. *Chem. Ber./Recl.* **1985**, *118*, 4665.

(14) de Silva, K. M. N.; Goodman, J. M. *J. Chem. Inf. Model.* **2005**, *45*, 81.

(15) Schreiner, P. R.; Chernish, L. V.; Gunchenko, P. A.; Tikhonchuk, E. Y.; Hausmann, H.; Serafin, M.; Schlecht, S.; Dahl, J. E. P.; Carlson, R. M. K.; Fokin, A. A. *Nature* **2011**, *477*, 308.

(16) (a) Schwertfeger, H.; Schreiner, P. R. *Chem. Unserer Zeit* **2010**, *44*, 248. (b) Schwertfeger, H.; Fokin, A. A.; Schreiner, P. R. *Angew. Chem., Int. Ed.* **2008**, *47*, 1022.

(17) Grimme, S.; Huenerbein, R.; Ehrlich, S. *ChemPhysChem* **2011**, *12*, 1258.

(18) Fokin, A. A.; Gerbig, D.; Schreiner, P. R. *J. Am. Chem. Soc.* **2011**, *133*, 20036.

(19) Fokin, A.; Schreiner, P. R. *Mol. Phys.* **2009**, *107*, 823.

(20) Sanvito, S. *Nat. Nanotechnol.* **2007**, *2*, 204.

(21) Grimme, S. *Wiley Interdiscip. Rev.: Comput. Mol. Sci.* **2011**, *1*, 211.

(22) (a) Grimme, S. *J. Comput. Chem.* **2006**, *27*, 1787. (b) Zhao, Y.; Schultz, N. E.; Truhlar, D. G. *J. Chem. Theory Comput.* **2006**, *2*, 364.

(23) Zhao, Y.; Truhlar, D. G. *Acc. Chem. Res.* **2008**, *41*, 157.

(24) (a) Woodcock, H. L.; Schaefer, H. F.; Schreiner, P. R. *J. Phys. Chem. A* **2002**, *106*, 11923. (b) Schreiner, P. R.; Fokin, A. A.; Pascal, R. A.; de Meijere, A. *Org. Lett.* **2006**, *8*, 3635. (c) Grimme, S. *Angew. Chem., Int. Ed.* **2006**, *45*, 4460. (d) Wodrich, M. D.; Corminboeuf, C.; Schreiner, P. R.; Fokin, A. A.; Schleyer, P. v. R. *Org. Lett.* **2007**, *9*, 1851. (e) Wodrich, M. D.; Corminboeuf, C.; Schleyer, P. v. R. *Org. Lett.* **2006**, *8*, 3631. (f) Schreiner, P. R. *Angew. Chem., Int. Ed.* **2007**, *46*, 4217.

(25) (a) Dahl, J. E.; Moldowan, J. M.; Peters, K. E.; Claypool, G. E.; Rooney, M. A.; Michael, G. E.; Mello, M. R.; Kohnen, M. L. *Nature* **1999**, *399*, 54. (b) Dahl, J. E.; Liu, S. G.; Carlson, R. M. K. *Science* **2003**, *299*, 96. (c) Dahl, J. E. P.; Moldowan, J. M.; Peakman, T. M.; Clardy, J. C.; Lobkovsky, E.; Olmstead, M. M.; May, P. W.; Davis, T. J.; Steeds, J. W.; Peters, K. E.; Pepper, A.; Ekuan, A.; Carlson, R. M. K. *Angew. Chem., Int. Ed. Engl.* **2003**, *42*, 2040.

(26) (a) Fokin, A. A.; Tkachenko, B. A.; Gunchenko, P. A.; Gusev, D. V.; Schreiner, P. R. *Chem.—Eur. J.* **2005**, *11*, 7091. (b) Fokin, A. A.; Schreiner, P. R.; Fokina, N. A.; Tkachenko, B. A.; Hausmann, H.; Serafin, M.; Dahl, J. E. P.; Liu, S.; Carlson, R. M. K. *J. Org. Chem.* **2006**, *71*, 8532. (c) Schreiner, P. R.; Fokina, N. A.; Tkachenko, B. A.; Hausmann, H.; Serafin, M.; Dahl, J. E. P.; Liu, S. G.; Carlson, R. M. K.; Fokin, A. A. *J. Org. Chem.* **2006**, *71*, 6709. (d) Tkachenko, B. A.; Fokina, N. A.; Chernish, L. V.; Dahl, J. E. P.; Liu; Carlson, R. M. K.; Fokin, A. A.; Schreiner, P. R. *Org. Lett.* **2006**, *8*, 1767. (e) Fokin, A. A.; Butova, E. D.; Chernish, L. V.; Fokina, N. A.; Dahl, J. E. P.; Carlson, R. M. K.; Schreiner, P. R. *Org. Lett.* **2007**, *9*, 2541. (f) Fokin, A.; Merz, A.; Fokina, N.; Schwertfeger, H.; Liu, S.; Dahl, J.; Carlson, R.; Schreiner, P. R. *Synthesis* **2009**, *2009*, 909. (g) Fokin, A. A.; Gunchenko, P. A.; Novikovsky, A. A.; Shubina, T. E.; Chernyaev, B. V.; Dahl, J. E. P.; Carlson, R. M. K.; Yurchenko, A. G.; Schreiner, P. R. *Eur. J. Org. Chem.* **2009**, *2009*, 5153. (h) Fokin, A. A.; Tkachenko, B. A.; Fokina, N. A.; Hausmann, H.; Serafin, M.; Dahl, J. E. P.; Carlson, R. M. K.; Schreiner, P. R. *Chem.—Eur. J.* **2009**, *15*, 3851. (i) Schreiner, P. R.; Fokin, A. A.; Reisenauer, H. P.; Tkachenko, B. A.; Vass, E.; Olmstead, M. M.; Blaser, D.; Boese, R.; Dahl, J. E. P.; Carlson, R. M. K. *J. Am. Chem. Soc.* **2009**, *131*, 11292. (j) Schwertfeger, H.; Würtele, C.; Hausmann, H.; Dahl, J. E. P.; Carlson, R. M. K.; Fokin, A. A.; Schreiner, P. R. *Adv. Synth. Catal.* **2009**, *351*, 1041.

(27) (a) Gund, T. M.; Nomura, M.; Schleyer, P. v. R. *J. Org. Chem.* **1974**, *39*, 2987. (b) Hollowood, F.; Karim, A.; McKervey, M. A.; McSweeney, P.; Duddeck, H. *J. Chem. Soc., Chem. Commun.* **1978**, 306. (c) Fokina, N. A.; Tkachenko, B. A.; Merz, A.; Serafin, M.; Dahl, J. E. P.; Carlson, R. M. K.; Fokin, A. A.; Schreiner, P. R. *Eur. J. Org. Chem.* **2007**, 4738.

(28) Dahl, J. E. P.; Moldowan, J. M.; Wei, Z.; Lipton, P. A.; Denisevich, P.; Gat, R.; Liu, S.; Schreiner, P. R.; Carlson, R. M. K. *Angew. Chem., Int. Ed.* **2010**, *49*, 9881.

(29) (a) Dunning, J.; Thom, H. *J. Chem. Phys.* **1989**, *90*, 1007. (b) Dunning, T. H., Jr. *J. Chem. Phys.* **1989**, *90*, 1007.

(30) (a) Becke, A. D. *Phys. Rev. A* **1988**, *38*, 3098. (b) Lee, C.; Yang, W.; Parr, R. G. *Phys. Rev. B* **1988**, *37*, 785.

(31) Becke, A. D. *J. Chem. Phys.* **1993**, *98*, 5648.

(32) Schmider, H. L.; Becke, A. D. *J. Chem. Phys.* **1998**, *108*, 9624.

(33) Grimme, S.; Antony, J.; Ehrlich, S.; Krieg, H. *J. Chem. Phys.* **2010**, *132*, 154104.

(34) Chai, J. D.; Head-Gordon, M. *Phys. Chem. Chem. Phys.* **2008**, *10*, 6615.

(35) Adamo, C.; Barone, V. *J. Chem. Phys.* **1999**, *110*, 6158.

(36) Perdew, J. P.; Burke, K.; Wang, Y. *Phys. Rev. B* **1996**, *54*, 16533.
(37) Iikura, H.; Tsuneda, T.; Yanai, T.; Hirao, K. *J. Chem. Phys.* **2001**, *115*, 3540.
(38) Zhao, Y.; Truhlar, D. G. *Theor. Chem. Acc.* **2008**, *120*, 215.
(39) van Nes, G. J. H.; Vos, A. *Acta Crystallogr., B* **1979**, *35*, 2593.
(40) Bartell, L. S.; Higginbotham, H. K. *J. Chem. Phys.* **1965**, *42*, 851.
(41) Duncan, J. L.; McKean, D. C.; Bruce, A. J. *J. Mol. Spectrosc.* **1979**, *74*, 361.
(42) Kahn, R.; Fourme, R.; Andre, D.; Renaud, M. *Acta Crystallogr., B* **1973**, *B 29*, 131.
(43) Ewbank, J. D.; Kirsch, G.; Schafer, L. *J. Mol. Struct.* **1976**, *31*, 39.
(44) Bartell, L. S.; Boates, T. L. *Acta Crystallogr.* **1966**, *S 21*, A103.
(45) Bartell, L. S.; Boates, T. L. *J. Mol. Struct.* **1976**, *32*, 379.
(46) Grimme, S. *J. Chem. Phys.* **2003**, *118*, 9095.
(47) Perdew, J. P. *Phys. Rev. B* **1986**, *33*, 8822.
(48) Becke, A. D. *J. Chem. Phys.* **1993**, *98*, 1372.
(49) Tsuzuki, S.; Luthi, H. P. *J. Chem. Phys.* **2001**, *114*, 3949.
(50) Miertus, S.; Scrocco, E.; Tomasi, J. *Chem. Phys.* **1981**, *55*, 117.
(51) Highly substituted alkanes generally prefer *gauche* over *anti* conformations, see Rüchardt, C.; Beckehaus, H.-D. *Angew. Chem., Int. Ed.* **1980**, *19*, 429−440.
(52) Moss, G. P. *Pure Appl. Chem.* **1996**, *68*, 2193.
(53) Previous attempts to measure the experimental rotational barrier around the CC bond for parent 1-(1-adamantyl)adamantane using (3-bromoadamantyl)-1-adamantane as a model were unsuccessful (Anderson, J. E.; de Meijere, A.; Kozhushkov, S. I.; Lunazzi, L.; Mazzanti, A. J. *Org. Chem.* **2003**, *68*, 8494). We determined a 8.0 kcal/mol barrier form variable temperature ^{13}C-NMR studies of 1-methyl-(3-methyl-1-adamantyl)adamantane.
(54) Wheeler, S. E.; Houk, K. N.; Schleyer, P. v. R.; Allen, W. D. *J. Am. Chem. Soc.* **2009**, *131*, 2547.
(55) Fokin, A. A.; Schreiner, P. R.; Schleyer, P. v. R.; Gunchenko, P. A. *J. Org. Chem.* **1998**, *63*, 6494.
(56) (a) Alden, R. A.; Kraut, J.; Traylor, T. G. *J. Am. Chem. Soc.* **1968**, *90*, 74. (b) Alden, R.; Kraut, J.; Traylor, T. G. *J. Phys. Chem.* **1967**, *71*, 2379.
(57) Engler, E. M.; Andose, J. D.; Schleyer, P. v. R. *J. Am. Chem. Soc.* **1973**, *95*, 8005.
(58) Grimme, S.; Muck-Lichtenfeld, C.; Erker, G.; Kehr, G.; Wang, H. D.; Beckers, H.; Willner, H. *Angew. Chem., Int. Ed.* **2009**, *48*, 2592.
(59) Jiemchooroj, A.; Sernelius, B. E.; Norman, P. *Phys. Rev. A* **2004**, *69*, 0447011.
(60) (a) Rohrer, J.; Hyldgaard, P. *Phys. Rev. B* **2011**, *83*, 165423. (b) Loktev, V. M.; Turkowski, V. *Low Temp. Phys.* **2011**, *164*, 264.
(61) (a) Nordman, C. E.; Schmitkons, D. L. *Acta Crystallogr.* **1965**, *18*, 764. (b) Roberts, P. J.; Ferguson, G. *Acta Crystallogr.* **1977**, *B33*, 2335. (c) Karle, I. L.; Karle, J. *J. Am. Chem. Soc.* **1965**, *87*, 918.
(62) (a) Yang, W. L.; et al. *Science* **2007**, *316*, 1460. (b) Clay, W. A.; Liu, Z.; Yang, W.; Fabbri, J. D.; Dahl, J. E.; Carlson, R. M. K.; Sun, Y.; Schreiner, P. R.; Fokin, A. A.; Tkachenko, B. A.; Fokina, N. A.; Pianetta, P. A.; Melosh, N.; Shen, Z.-X. *Nano Lett.* **2009**, *9*, 57.
(63) Wen, X. D.; Hand, L.; Labet, V.; Yang, T.; Hoffmann, R.; Ashcroft, N. W.; Oganov, A. R.; Lyakhov, A. O. *Proc. Natl. Acad. Sci. U.S.A.* **2011**, *10*, 6833.
(64) Kruger, A.; Kataoka, F.; Ozawa, M.; Fujino, T.; Suzuki, Y.; Aleksenskii, A. E.; Vul', A. Y.; Osawa, E. *Carbon* **2005**, *43*, 1722.
(65) Cudazzo, P.; Tokatly, I. V.; Rubio, A. *Phys. Rev. B* **2011**, *84*, 085406.
(66) (a) Zutic, I.; Fabian, J.; Sarma, S. D. *Rev. Mod. Phys.* **2004**, *76*, 323. (b) Naber, W. J. M.; Faez, S.; van der Wiel, W. G. *J. Phys. D: Appl. Phys.* **2007**, *40*, R205.
(67) Maier, F.; Riedel, M.; Mantel, B.; Ristein, J.; Ley, L. *Phys. Rev. Lett.* **2000**, *85*, 3472.
(68) Frisch, M. J. et al.; *Gaussian09*, version B.01; Gaussian, Inc.: Wallingford, CT, 2010.
(69) Schmidt, M. W.; Baldridge, K. K.; Boatz, J. A.; Elbert, S. T.; Gordon, M. S.; Jensen, J. H.; Koseki, S.; Matsunaga, N.; Nguyen, K. A.; Su, S. J.; Windus, T. L.; Dupuis, M.; Montgomery, J. A. *J. Comput. Chem.* **1993**, *14*, 1347.
(70) Neese, F., with contributions from Becker, U.; Ganiouchine, D.; Kossmann, S.; Petrenko, T.; Riplinger, C.; Wennmohs, F.; *ORCA*, version 2.8.0; Max-Planck Institute for Bioinorganic Chemistry: Mülheim an der Ruhr, Germany, 2011.
(71) (a) Sheldrick, G. M. Universität Göttingen, 1997; (b) Sheldrick, G. M. *Acta Crystallogr.* **2008**, *A64*, 112.